Available online at www.sciencedirect.com
ScienceDirect
Progress in Natural Science: Materials International 21(2011) 40−45
Progress in Natural Science: Materials International
www.elsevier.com/locate/pnsc

First-principles simulation and experimental evidence for improvement of transmittance in ZnO films

Dong-yan ZHANG[1, 2], Pang-pang WANG[1, 2], Ri-ichi MURAKAMI[2], Xiao-ping SONG[1]

1. State Key Laboratory for Mechanical Behavior of Materials, Key Laboratory for Nonequilibrium Synthesis and Modulation of Condensed Matter, Ministry of Education, Xi'an Jiaotong University, Xi'an 710049, China;
2. Department of Mechanical Engineering, The University of Tokushima, 2-1 Minamijosanjima-cho, Tokushima 770-8506, Japan

Received 23 October 2010; accepted 23 December 2010

Abstract: ZnO/Ag/Glass films were prepared by a DC magnetron sputtering system, which exhibit both excellent properties of high conductivity and high transparency. Moreover, an enhancement of transmission of ZnO films was observed after brought into contact to a silver layer, but the understanding of experimental findings for the enhancement of transmission was insufficient. Therefore, the first-principles simulations of electrical and optical properties were utilized using the density functional theory with local-density approximations or generalized-gradient approximations. The crystal structure of ZnO or Ag was imported from the Material Studio database. The periodic supercell has the same atomic ratio with the experimental structure and was optimized using the CASTEP package in Material Studio. According to the calculation results, the enhancement in transmission is attributed to the surface plasmon polariton in the asymmetric structure films.
Key words: first-principles; transparent conductive oxide; ZnO; transmittance; surface plasmon polaritons

1 Introduction

ZnO is one of the most attractive metal oxides for next-generation semiconductor electronics due to its unique properties such as a direct band gap (≤3.4 eV), a large exciton binding energy (≤60 meV)[1]. Recently, ZnO with embedded metal layer is a promising transparent conductive oxide (TCO) film applied in electronic devices[2−7], such as light emitting devices, low emissivity windows, solar cells, and flexible electronics. Indium tin oxide (ITO), the current commercial TCO for optoelectronics, is becoming rare and expensive[8]. Thus, there is an urgent need for new TCO materials. ZnO films with embedded metal layer exhibit good electrical conductivity and optical transmission in the visible region. ZnO also has practical advantages such as nontoxic, inexpensive and abundant in earth[9]. ZnO with embedded films is the optical coating designed for transparent electrodes which have high conductivity without significant decline in optical transmission. To achieve this effect, the coating also contains a thin layer of metal, usually, silver, to be embedded in the film. The technologies for synthesizing ZnO/metal/ZnO films are also improved greatly, such as chemical spray pyrolysis, metal-organic chemical vapor deposition, radical source-MBE, sol-gel process, and magnetron sputtering. Using the magnetron sputtering method, a bottom ZnO (002) layer was prepared to encourage Ag mid layer textured growth in the low-energy (111) orientation, and then a top ZnO layer was sputtered. In addition, ZnO-Ag contact was investigated[10]. Since ZnO adopts the wurtzite (hexagonal) crystal form, there are distinct sites aligned along the *c* axis of the material. Therefore, it is important to characterize the ZnO-Ag interface at the atomic level, and possibly modify the synthesis method to improve its properties for transparent electrode.

Various studies were done on the improvement of transmission and conductivity of Ag-embedded ZnO films. SIVARAMAKRISHNAN et al[5, 11−13] investigated the mechanism of carrier transport in ZnO with embedded Ag or Au layer and the role of copper in ZnO/Cu/ZnO thin films. CHO et al[14] and JEONG et al[15] compared the electrical, optical, structural, and interface properties of doped ZnO with embedded noble

Corresponding author: Ri-ichi MURAKAMI; E-mail: murakami@me.tokushima-u.ac.jp; Xiao-ping SONG; E-mail: xpsong@mail.xjtu.edu.cn

metal layer, as well as the dependence of their electrical and optical properties on the thickness of the metal layer when used for organic solar cells. LI et al[16] studied the effect of silver growth temperature on the contacts with ZnO thin films. Also, first-principles studies on ZnO films were done. LIN et al[17−19] investigated the microscopic properties of the Ag (111)/ZnO (0001) interface by first-principles computational method. YANG et al[20] investigated the structures and optical properties of ZnO nanowire by ab initio calculations of the pseudo-potential density functional method. DONG and BRILLSON[21] studied the atomic and electronic structures for various metal (111)/ZnO (111) interfaces by first-principles calculations based on density functional theory and found that the Schottky barrier heights at metal/ZnO were very sensitive to the specific interface chemical bonding. In present work, the structure and optical properties of ZnO (002) layer contacted with Ag (111) were calculated and the evidence of enhanced optical transmission for ZnO/Ag/ZnO films was presented. The mechanism of the optical transmission enhancement through a ZnO film with embedded Ag was also discussed by considering the deformation charge density and difference charge density. The surface plasmon resonance (SPR) at the Ag-ZnO interface was taken into account. The ohmic contact model, the Drude free electron model and a density function theory were used to investigate the optical enhancement.

To study the optical properties of ZnO contacted with Ag, it is necessary to specify the structure of the ZnO surface and build a supercell. X-ray diffraction results indicate that ZnO films have the wurtzite structure with polar (002) surfaces. In the DC magnetron sputtering experiments, ZnO was first deposited onto the glass quartz substrate, and Ag was deposited onto the ZnO (002) surface, grew in the (111) orientation, and formed three-dimensional islands. In our previous study, the formation of islands-plus-layered mode was proved (Stranski-Krastanov mode)[22]. In addition to ZnO and Ag surface model, there is another problem to build the Ag-ZnO contact model. The bulk lattice parameters for the 1×1 ZnO (002) and Ag (111) surfaces are 3.25 Å[23] and 2.89 Å[24], respectively. Therefore, the mismatch between ZnO lattice parameters and Ag lattice parameters is too large for the geometry optimization by first principle calculation. A 30° rotated epitaxial relationship was assumed. A $1\times3^{-1/2}$ ZnO (002) unit cell with the lattice parameters 6.50 Å×5.63 Å was built. Therefore, the present work focused on such an ideal interface.

2 Experimental

In this work, the CASTEP toolkit package[25] was employed to perform the geometry optimization and the band structure, density of states, and optical properties calculation. The plane-wave ultrasoft pseudopotential method based on density functional theory (DFT) was used as basic set of wave function. The cut-off kinetic-energy of plane wave was 300 eV and the convergence of energy change was less than 3×10^{-5} eV/atom. The generalized gradient approximation (GGA) for the exchange correlation energy was chosen, rather than the local density approximation (LDA), due to its superior band structure calculation[26]. The GGA using the Perdew, Burke, and Ernzerhof[27] (PBE) functional was chosen for the calculations. The optimization convergence for energy change, maximum displacement, maximum stress, and maximum displacement were set at 3×10^{-5} eV/atom, 0.05 eV/Å, 0.1 GPa, and 0.002 Å, respectively. The optimization step stopped until all the convergence conditions were satisfied. The structure of ZnO supercell with 5 atoms (2 oxygen atoms and 3 zinc atoms) was imported from the inorganic crystal structure database (ICDS). The lattice parameters were a=b=3.25 Å, c=5.21 Å, α=β=90°, γ=120°. The supercell was cleaved at (002) surface. The surface vectors U was along (110), and V was along (−110). From the surface, 4-fractional depth (20.822 Å) was extended. The lattice parameters for the cleaved surface cell were u=3.25 Å, v=5.63 Å, θ=90°. The U orientation was along X axis, and V orientation was in the XY plane. Such a cleaved ZnO structure was employed to assemble a ZnO/Ag multilayer and Ag atom diffusion model.

The ZnO/Ag/ZnO multilayer films were prepared using a DC magnetron sputtering system (NACHI, SP−1530−1) at room temperature. Pure silver (99.99%) and Zn (99.99%) were used as targets, respectively. The Ag layer was deposited under argon (50 cm^3/min at STP) atmosphere. The ZnO layer was deposited under argon (50 cm^3/min) mixed with oxygen (3 cm^3/min). Before argon or oxygen was injected, the chamber pressure would be kept at about 3×10^{-3} Pa. Under this condition (listed in Table 1), the growth rate of Ag layer was at 0.2 nm/s, and that of ZnO layer was very low at 0.5 nm/min as a result of the addition of oxygen. Therefore, the thickness of each layer was determined by the sputtering time. A series of samples were prepared as listed in Table 2. The Ag sputtering time was set at 10, 20, 30 and 40 s, and the thicknesses of Ag layer were 2, 4, 6 and 8 nm. The sputtering time of ZnO layer was set at 50 min, and the thickness of ZnO layer was 25 nm. In comparing, a single layer ZnO was also sputtered for 50−50 min. It has

been proven in our previous work that the Ag layer is not smooth but has a layer-plus-island nanostructure. The random Ag islands act as a grating with a random grating constant. The optical transmittance spectrum was measured by a UV-Vis spectrometer (JASCO, V570) in a wavelength range of 300−800 nm. The crystalline structures of the ZnO films with embedded Ag were studied using X-ray diffraction (XRD, Rigaku-RINT 2500) with Cu K_α radiation operating at 40 kV and 40 mA, and the data were collected with a step size of 0.02º and scanning speed of 4 (º)/min. Photoluminescence (PL) measurements were carried out in reflection at a 45° incident angle using a fluorescence spectrophotometer (HITACHI, F−7000).

Table 1 Sputtering parameters for ZnO and Ag layers

Layer type	Ar flow/ ($cm \cdot min^{-1}$)	O_2 flow/ ($cm \cdot min^{-1}$)	Current/ A	Voltage/ V	Growth time	Growth rate/ ($nm \cdot min^{-1}$)
ZnO	50	3	0.1	250	3 000	0.5
Ag	50	0	0.4	280	10, 20, 30, 40	12

Table 2 Thickness of each layer for samples (nm)

Sample No.	Layer structure	Top ZnO layer	Ag	Bottom ZnO layer
A	ZnO/Ag/ZnO	25	2	25
B	ZnO/Ag/ZnO	25	4	25
C	ZnO/Ag/ZnO	25	6	25
D	ZnO/Ag/ZnO	25	8	25

3 Results and discussion

In order to build up a ZnO-Ag contact model, the growth orientation of Ag and ZnO layers had to be specified. Fig.1 shows the XRD patterns of ZnO films with embedded Ag layer. XRD analysis indicates that all ZnO films have a fine-grained hexagonal structure. A strong preferred (002) peak is seen for ZnO in all samples. Strong preferential orientation indicates growth (002) direction of ZnO layers perpendicular to the substrate. The growth orientation of ZnO is the experimental evidence to cleave (002) surface of ZnO supercell in the first principles study. With increasing the thickness of Ag layer, the intensity of (111) peak increases, and that of ZnO (002) is stable. This means that the crystalline structure of bottom ZnO layer does not transform with the mid Ag layer sputtering. The mass Ag film growing on a crystal surface or interface under special preparing conditions should follow the Stranski-Krastanov growth mechanism[28], a layer-plus-islands growth model. In our case, the ZnO bottom layer has a crystalline structure, and the sputtering conditions (as listed in Table 1) for Ag layer growth make the layer-plus-islands structure feasible. The XRD analysis of ZnO films with embedded Ag layer indicates that the ZnO-Ag contact model has to be built to make the (111) Ag along the (002) ZnO crystalline orientation. Furthermore, in order to build Ag (111)/ZnO (002) interface, the ZnO growth model along (002) orientation and the special positions of the two crystals at the interface plane have to be illustrated. The Ag atoms can be placed on the ZnO surface at three different high-symmetry adsorption sites, face-central-cubic (fcc) hollow site, hexagonal closed packed hollow site, and on top site.

Figure 2 shows the schematic of the supercell used to construct the Ag-ZnO interface. In order to construct Ag-ZnO interface model, the in-plane lattice parameters

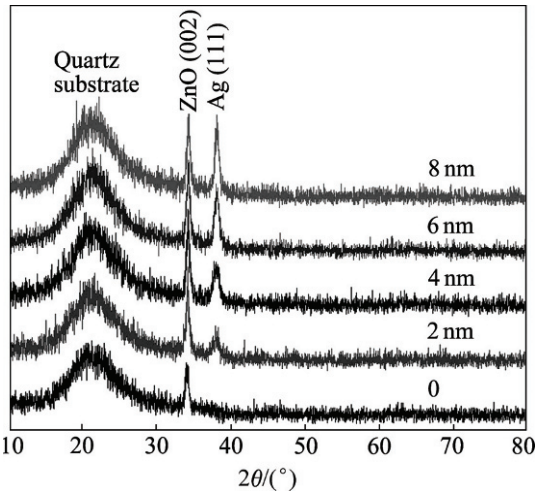

Fig.1 XRD patterns of ZnO films with embedded Ag layer

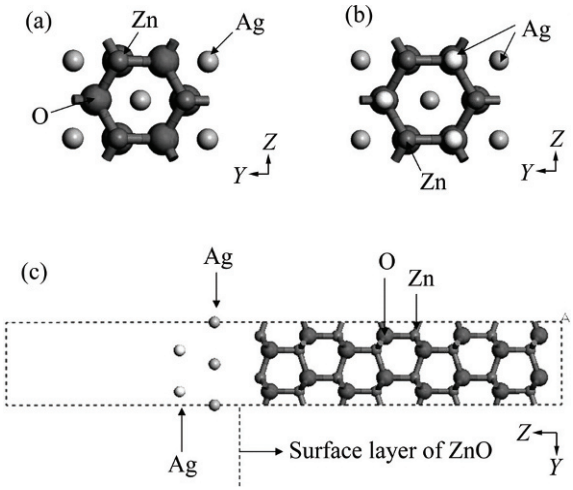

Fig.2 Schematic of supercell to construct Ag-ZnO interface: (a) Top view of one layer Ag atoms occupied fcc hollow sites on ZnO surface; (b) Top view of two layer Ag atoms placed on ZnO interface; (c) Side view of Ag-ZnO interface model

of Ag were increased so that they matched with the lattice parameters of ZnO. After the geometry optimization using the CASTEP toolkit package, the electronic band structures of this model were studied. The band structure and density of states of ZnO and Ag-ZnO interface were studied based on the geometry optimization. The band gap was sheared by a scissors operator according to the photoluminescence spectra (shown in Fig.3). Fig.4 represents the band structure and DOS of ZnO and Ag-ZnO interface.

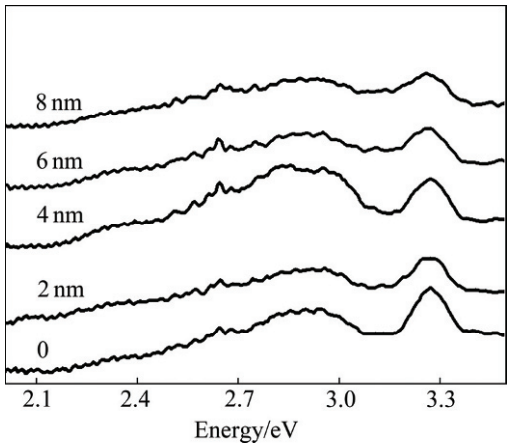

Fig.3 PL spectra for ZnO/Ag/ZnO films with different thicknesses of Ag layer

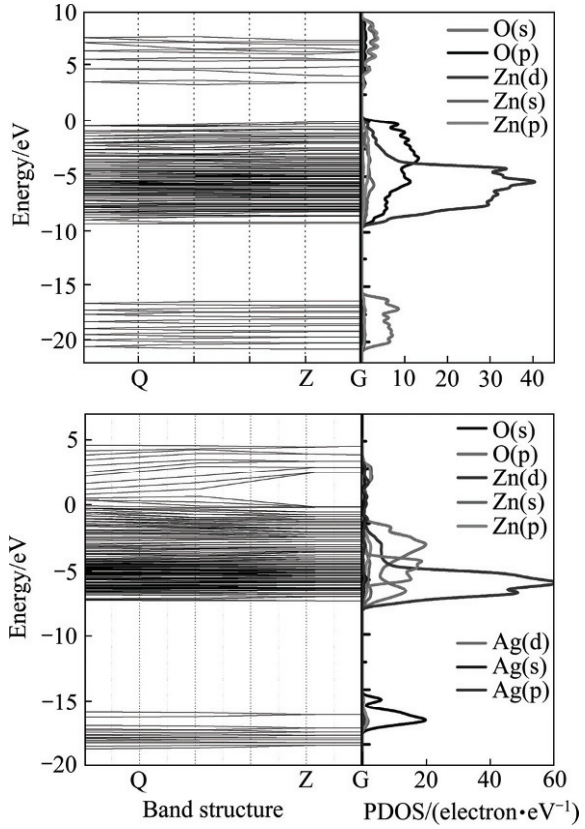

Fig.4 Band structure and density of states of ZnO and ZnO-Ag interface

Optical properties are calculated by CASTEP from the dielectric function, and the imaginary part of which can be calculated directly from the full many-electron wave function. Since the dielectric constant describes a causal response, the real and imaginary parts are linked by a Kramers-Kronig transform. The real part can be obtained via the Kramers-Kronig relationship. The refractive index can be calculated using the following equation:

$$\begin{cases} N^2 = \varepsilon_1 + \mathrm{i}\varepsilon_2 \\ N = n + \mathrm{i}k \end{cases} \tag{1}$$

where N is the complex refractive index, ε_1 and ε_2 are the real and imaginary parts of the dielectric function, n and k are the real and imaginary parts of the refractive index, respectively. The imaginary and real parts of the refractive index are calculated along the incident direction (002). The DFT underestimates the band gap, which will lead to a significant error. However, this error can be removed by a scissors operator. A 3.3 eV scissors operator is exerted when the optical properties were calculated. Fig.5 shows the refractive index of ZnO before and after bringing contact with Ag. Both the real and imaginary parts of the refractive index are shrunk. The reflection coefficient can be obtained for the simple case of normal incidence onto a plane surface by matching both the electric and magnetic fields on the surface as the following equation:

$$R = \left|\frac{1-N}{1+N}\right|^2 = \frac{(n-1)^2 + k^2}{(n+1)^2 + k^2} \tag{2}$$

where R is the reflection coefficient. A shrunk refractive index indicates a reduced reflection coefficient and an enhanced transmission. The imaginary part of the refractive index is related to the absorption coefficient as follows:

$$\eta = \frac{2k\omega}{c} \tag{3}$$

where η is the absorption coefficient, ω is the angular frequency, and c is the velocity of light in vacuum. The absorption coefficient indicates the fraction of energy lost by the wave when passing through a certain material. A shrunk imaginary part of the refractive index leads to a reduced absorption and an enhanced transmission. Otherwise, when ZnO and Ag are brought into contact, electrons are transferred from Ag to ZnO to align the Fermi level. Because of electron transfer, an interface charge density wave is expected at the Ag-ZnO interface, acting as surface plasmon. If a coherent oscillation occurs between the surface plasmon and incident light, a harmonic, which enhances the transmittance, is generated. In our previous studies[29−30], the Ag layer

is a layer-plus-island structure rather than a perfect flat layer. The random Ag islands can be thought as a grating with a random grating constant, α, to offer a wave vector for coupling incident light with surface plasmon. Therefore, an electron band structure calculation and an expected interface charge density wave will enhance the transmission.

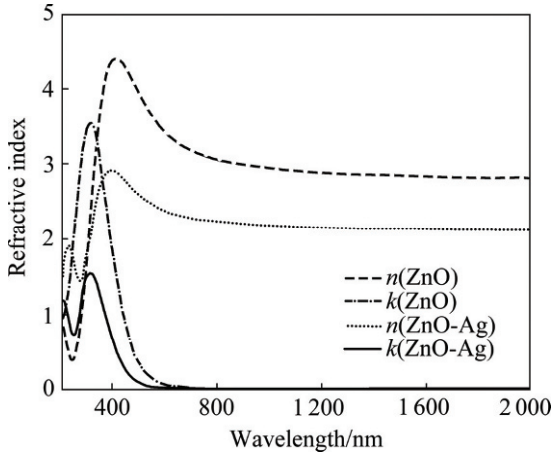

Fig.5 Complex refractive index of ZnO and ZnO-Ag

ZnO films with embedded Ag layer are expected to have an enhanced transmission according to the first-principles calculation. The optical transmittance spectrum was measured by a UV-Vis spectrometer in a wavelength range of 300−800 nm. An enhanced transmittance is observed over the ZnO films as shown in Fig.6. In addition, the electrical conductivity of ZnO films with embedded Ag is significantly improved over the ZnO films. The resistivity of ZnO films with embedded 2 nm Ag layer is 1.32×10^{-4} Ω·cm. This improvement of electrical conductivity can be explained by the first-principle calculation. In Fig.4, the partial density of states for Zn atom at ZnO-Ag interface indicates an electron transfer from Ag to ZnO and the energy band is split near the Fermi level.

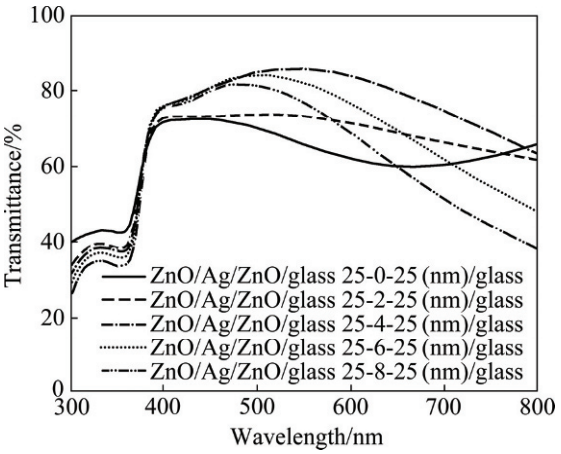

Fig.6 Transmittance of ZnO films with embedded Ag layer

4 Conclusions

1) The partial density of states calculation indicates an improvement of electrical conductivity. This suggests that the diversification of resistivity as a function of Ag thickness is nonlinear.

2) According to the band structure calculation, the real and imaginary parts of the refractive index are reduced, which weaken the reflection coefficient and absorption coefficient.

3) The transmittance spectra of ZnO films with embedded Ag are enhanced over that of ZnO films.

4) The dielectric function calculation and surface plasmon polariton model suggest an enhanced transmission, and experimental evidence of enhanced transmission is given.

Acknowledgments

This study was supported by the Double Degree Program (DDP) of The University of Tokushima and by the Ministry of Education, Culture, Sports, Science & Technology (MEXT), Japan. The authors would like to thank Dr. Pankaj Koinkar of the University of Tokushima for English correction.

References

[1] RYU Y R, LEE T S, LUBGUBAN J A, et al. ZnO devices: Photodiodes and p-type field-effect transistors[J]. Applied Physics Letters, 2005, 87(15): 153504−3.

[2] KLINGSHIRN C. ZnO: From basics towards applications[J]. Physica Status Solidi B, 2007, 244(9): 3027−3073.

[3] SAHU D R, LIN S Y, HUANG J L. ZnO/Ag/ZnO multilayer films for the application of a very low resistance transparent electrode[J]. Applied Surface Science, 2006, 252(20): 7509−7514.

[4] KIM D, YUN I, KIM H. Fabrication of rough Al doped ZnO films deposited by low pressure chemical vapor deposition for high efficiency thin film solar cells[J]. Current Applied Physics, 2010, 10(S1): 459−462.

[5] SIVARAMAKRISHNAN K, ALFORD T L. Conduction and transmission analysis in gold nanolayers embedded in zinc oxide for flexible electronics[J]. Applied Physics Letters, 2010, 96(20): 201109−3.

[6] MÜLLER J, RECH B, SPRINGER J. TCO and light trapping in silicon thin film solar cells[J]. Solar Energy, 2004, 77(6): 917−930.

[7] LOOK D C, LEEDY K D, TOMICH D H, BAYRAKTAROGLU B. Mobility analysis of highly conducting thin films: Application to ZnO[J]. Applied Physics Letters, 2010, 96(6): 062102−3.

[8] CHIPMAN A. A commodity no more[J]. Nature, 2007, 449(7159): 131−131.

[9] PARK T Y, CHOI Y S, KANG J W, et al. Enhanced optical power and low forward voltage of GaN-based light-emitting diodes with Ga-doped ZnO transparent conducting layer[J]. Applied Physics Letters, 2010, 96(5): 051124−3.

[10] RYU Y R, ZHU S, LOOK D C, et al. Synthesis of p-type ZnO films[J]. Journal of Crystal Growth, 2000, 216(1/4): 330−334.

[11] HAN H, THEODORE N D, ALFORD T L. Improved conductivity and mechanism of carrier transport in zinc oxide with embedded silver layer[J]. Journal of Applied Physics, 2008, 103(1): 013708−8.

[12] SIVARAMAKRISHNAN K, ALFORD T L. Metallic conductivity and the role of copper in ZnO/Cu/ZnO thin films for flexible

electronics[J]. Applied Physics Letters, 2009, 94(5): 052104−3.

[13] SIVARAMAKRISHNAN K, THEODORE N D, MOULDER J F. The role of copper in ZnO/Cu/ZnO thin films for flexible electronics[J]. Journal of Applied Physics, 2009, 106(6): 063510−8.

[14] CHO S W, JEONG J A, BAE J H, et al. Highly flexible, transparent, and low resistance indium zinc oxide-Ag-indium zinc oxide multilayer anode on polyethylene terephthalate substrate for flexible organic light light-emitting diodes[J]. Thin Solid Films, 2008, 516(21): 7881−7885.

[15] JEONG J A, PARK Y S, KIM H K. Comparison of electrical, optical, structural, and interface properties of IZO-Ag-IZO and IZO-Au-IZO multilayer electrodes for organic photovoltaics[J]. Journal of Applied Physics, 2010, 107(2): 023111−8.

[16] LI X K, LI Q S, LIANG D C, et al. Effect of silver growth temperature on the contacts between Ag and ZnO thin films[J]. Science in China Series E-Technological Sciences, 2009, 52(9): 2779−2784.

[17] LIN Z, BRISTOWE P D. Microscopic characteristics of the Ag (111)/ZnO (0001) interface present in optical coatings[J]. Physical Review B, 2007, 75(20): 205423.

[18] LIN Z, BRISTOWE P D. A density functional study of the effect of hydrogen on the strength of an epitaxial Ag/ZnO interface[J]. Journal of Applied Physics, 2007, 102(10): 103513−6.

[19] LIN Z, BRISTOWE P D. A first principles study of the properties of Al:ZnO and its adhesion to Ag in an optical coating[J]. Journal of Applied Physics, 2009, 106(1): 013520−10.

[20] YANG Y R, YAN X H, XIAO Y, et al. The optical properties of one-dimensional ZnO: A first-principles study[J]. Chemical Physics Letters, 2007, 446(1/3): 98−102.

[21] DONG Y F, BRILLSON L J. First-principles studies of metal (111)/ZnO{0001} interfaces[J]. Journal of Electronic Materials, 2008, 37(5): 743−748.

[22] BAUER E. Phänomenologische theorie der Kristallabscheidung an Oberflächen. I[J]. Zeitschrift für Kristallographie, 2010, 110(1/6): 372−394.

[23] XU Y N, CHING W Y. Electronic, optical, and structural properties of some wurtzite crystals[J]. Physical Review B, 1993, 48(7): 4335.

[24] SMAKULA A, KALNAJS J. Precision determination of lattice constants with a geiger-counter X-ray diffractometer[J]. Physical Review, 1955, 99(6): 1737−1743.

[25] SEGALL M D, LINDAN P J D, PROBERT M J, et al. First-principles simulation: ideas, illustrations and the CASTEP code[J]. Journal of Physics: Condensed Matter, 2002, 14(11): 2717−2744.

[26] CARLING K, WAHNSTRÖM G, MATTSSON T R, et al. Vacancies in metals: From first-principles calculations to experimental data[J]. Physical Review Letters, 2000, 85(18): 3862−3865.

[27] PERDEW J P, BURKE K, ERNZERHOF M. Generalized gradient approximation made simple[J]. Physical Review Letters, 1996, 77(18): 3865−3868.

[28] MULLER T, NIENHAUS H. Ultrathin Ag films on H:Si(111)-1×1 surfaces deposited at low temperatures[J]. Journal of Applied Physics, 2003, 93(2): 924−929.

[29] WANG P, ZHANG D Y, KIM D H, et al, Enhancement of light transmission by coupling to surface plasmon polaritons of a layer-plus-islands silver layer[J]. Journal of Applied Physics, 2009, 106(10): 103104−5.

[30] ZHANG D, WANG P P, MURAKAMI R I, et al. Effect of an interface charge density wave on surface plasmon resonance in ZnO/Ag/ZnO thin films[J]. Applied Physics Letters, 2010, 96(23): 233114−3.